JOURNAL OF CATALYSIS 67, 103–109 (1981)

SCF–SW–Xα Studies of Octahedral Clusters in Molybdenum Oxides

II. Double Octahedra[1]

EWA BROCLAWIK,[2] ANIKO E. FOTI,[3] AND VEDENE H. SMITH JR.

Department of Chemistry, Queen's University, Kingston, Ontario K7L 3N6, Canada

Received March 19, 1980; revised July 14, 1980

SCF–SW–Xα calculations for $[Mo_2O_{11}]^{10-}$, $[Mo_2O_{11}]^{14-}$, and $[Mo_2O_{10}]^{12-}$ are reported. The interpretation of inner-shell photoelectron spectra of reduced MoO_3 is suggested: namely, that the molybdenum oxidation number is lowered from +6 to +4 without a change of crystal structure in the first stage of reduction while the structure changes from corner-linked zig-zag strings of octahedra to clusters of edge-sharing octahedra in the second.

1. INTRODUCTION

The structure and chemical bonding in molybdenum oxides are still of great interest because of the catalytic properties of molybdenum compounds. Additionally on the basis of available data molybdenum should be considered to be the most prolific of all the metallic elements in the formation of homonuclear metal–metal bonds (*1*). There are known species containing single to quadruple molybdenum–molybdenum bonds (*1*, *2*). However, there are only a very few possible cases of double bonding between molybdenum atoms. Although the existence of Mo═Mo bonds is perhaps more certain in Mo_2(O-Bu-t)$_6$(CO) (*3*) and Mo_2(O-i-Pr)$_8$ (*4*), it is certainly possible that such a bond exists in MoO_2 in which pairs of Mo atoms, each surrounded by an octahedron of oxygen atoms, are separated by only a small distance (*1*).

In a previous paper (*5*), we have reported the results of calculations of the electronic structure of molybdenum oxides which were carried out by means of the SCF–SW–Xα method (*6–8*) with the assumption of a simple geometrical model for the cluster, namely one metal atom surrounded by an octahedron of six oxygen atoms. The main purpose of that work was to discriminate between two contradictory experimental correlations of the molybdenum 3*d* binding energy and the formal oxidation number of the metal (*9–10*). Such a model (*5*) was able to give a semiqualitative interpretation of Mo 3*d* binding energy shifts during the course of reduction of MoO_3 in terms of formation of Mo^{6+}, Mo^{4+}, and Mo^{2+} ions.

We have now carried out SCF–SW–Xα calculations for two adjacent Mo–O octahedra in order to take into account more features of the real molybdenum oxide crystal structure and to get some information about metal–metal interactions. We have chosen two clusters of corner-linked octahedra, $[Mo_2O_{11}]^{10-}$ and $[Mo_2O_{11}]^{14-}$, and one cluster of edge-linked octahedra, $[Mo_2O_{10}]^{12-}$, as the representatives of the substrates and the products of reduction of MoO_3 in the two steps of the reduction process, respectively. Results of our calculations reported in this paper support our prediction (*5*) that in the first step of reduction, a simple reduction of Mo^{6+} ion to Mo^{4+} ion without a change of geometrical structure occurs whereas the rearrangement

[1] Research supported in part by the Natural Sciences and Engineering Research Council of Canada and by the Advisory Research Committee of Queen's University.

[2] Permanent address: Institute of Catalysis and Surface Chemistry, Polish Academy of Sciences, Krakow, Poland.

[3] Present address: Department of Chemistry, University of Montreal, Montreal, Quebec, Canada.

0021-9517/81/010103-07-$02.00/0

of geometry leading to molybdenum–molybdenum bond formation happens next.

2. METHOD OF CALCULATION AND PARAMETER CHOICE

The calculations for all the molybdenum–oxygen clusters have been carried out by the SCF–SW–Xα method in the muffin-tin approximation (*6–8*). This method has proven to be capable of accurately describing the electronic structure of quite large inorganic molecules and clusters (*2, 12–15*). The principles of the method have been discussed in the papers just mentioned and we will not go into them here. We decided to perform spin-restricted calculations since the exchange polarization was found to be relatively small in similar cases (*12–15*). We used the frozen core approximation in the first step of the calculations but later the molybdenum 1*s*, 2*s*, 2*p*, 3*s*, 3*p*, 3*d*, and oxygen 1*s* core orbitals were permitted to relax and to adjust their orbital energies during the self-consistent procedure. The converged ground-state potential was used to search for the virtual levels. This potential was used as a starting point for the SCF calculation of the Mo 3*d* ionization energy according to Slater's transition-state technique (*7*).

An idealized geometrical model for the double-octahedral clusters was assumed in which each of two molybdenum atoms was surrounded by a regular octahedron of oxygen atoms. The metal–oxygen bond length in MoO_3 could be easily found from the crystal-lattice parameters as 2.431 Å (*16*). $[Mo_2O_{11}]^{10-}$ and $[Mo_2O_{11}]^{14-}$ clusters were constructed from two corner-linked octahedra with one oxygen atom shared and formal molybdenum oxidation number equal to +6 and +4, respectively. The $[Mo_2O_{10}]^{12-}$ cluster was built from two edge-linked octahedra with two oxygen atoms shared and molybdenum atoms displaced from the octahedral centers corresponding to a shorter molybdenum–molybdenum distance equal to 2.50 Å reported in (*17*). Both arrangements of double octahedra and coordinate choice are presented in Fig. 1.

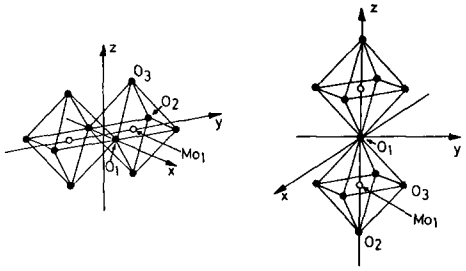

FIG. 1. Geometrical structure of $[Mo_2O_{10}]^{12-}$ and $[Mo_2O_{11}]^{n-}$.

Sphere radii in the muffin-tin approximation were chosen according to the "touching-spheres" requirement. The ratio of radii for molybdenum and oxygen was chosen according to the ratio of Slater's atomic radii (*18*). Throughout the calculations the stabilizing influence of a surrounding crystal lattice on the ions was simulated by adding to the potential that of a "Watson sphere" (*19*) containing 10, 14, and 12 units of positive charge, respectively, uniformly distributed over its surface, with radius equal to that of the outer sphere. The atomic values of the exchange parameter α were taken from (*20*); for the inter-sphere

TABLE 1

Atomic Coordinates, α Parameters, and Sphere Radii for $[Mo_2O_{10}]^{12-}$ and $[Mo_2O_{11}]^{n-}$ (Nonequivalent Atoms Only, Atomic Units)

Atom	*x*	*y*	*z*	*R*	α
			$[Mo_2O_{10}]^{12-}$		
Out	0.0	0.0	0.0	6.7042	0.744
Mo	0.0	2.3435	0.0	2.3435	0.703
O_1	2.9290	0.0	0.0	1.4076	0.744
O_2	2.4565	4.9130	0.0	1.2113	0.744
O_3	0.0	2.4565	3.6850	1.3442	0.744
			$[Mo_2O_{11}]^{n-}$		
Out	0.0	0.0	0.0	10.5368	0.744
Mo	0.0	0.0	−4.5954	1.3460	0.703
O_1	0.0	0.0	0.0	1.3460	0.744
O_2	0.0	0.0	−9.1908	1.3460	0.744
O_3	0.0	4.5954	−4.5954	1.3460	0.744

region a weighted average α was used where the weights were the number of atoms; the outer-sphere α value was equal to that of oxygen. Coordinates for non-equivalent atoms, α parameters, and sphere radii are summarized in Table 1. Full D_{4h} symmetry was used to factor the secular matrix in the case of $[Mo_2O_{11}]^{n-}$ clusters and D_{2h} symmetry was used in the case of $[Mo_2O_{10}]^{12-}$.

3. GROUND-STATE ELECTRONIC STRUCTURE AND CHEMICAL BONDING

The results of the calculations of the ground-state energy levels are presented in Table 2 for $[Mo_2O_{11}]^{n-}$ and in Table 3 for $[Mo_2O_{10}]^{12-}$. Only the higher energy levels are listed. The lower levels consist of the nearly pure Mo 4*s*, Mo 4*p*, and O 2*s* bands uniformly shifted with respect to atomic levels and showing only small splitting of each band. For the levels under consideration the metal contribution (calculated from the fraction of the charge located in the metal spheres) is listed and for those levels having more than 20% molybdenum character the major spherical harmonic basis function on Mo is given.

Inspection of Tables 2 and 3 shows that the valence energy levels for different forms of molybdenum oxide can be dis-

TABLE 2

Energies (Ry) and Metal Contributions of the Ground-State Upper Valence Levels for $[Mo_2O_{11}]^{10-}$ and $[Mo_2O_{11}]^{14-}$

$[Mo_2O_{11}]^{10-}$				$[Mo_2O_{11}]^{14-}$			
Level	$-E$ (Ry)	$2Q_{Mo}$ (%)	Major Mo (l,m)	Level	$-E$ (Ry)	$2Q_{Mo}$ (%)	Major Mo (l,m)
$6e_u$	0.295	58	$d_{xz} - d_{xz}$	$6e_u$	0.083	60	$d_{xz} - d_{xz}$
$2b_{1u}$	0.297	44	$d_{xy} - d_{xy}$	$2b_{1u}$	0.085	60	$d_{xy} - d_{xy}$
$2b_{2g}$	0.298	60	$d_{xy} + d_{xy}$	$2b_{2g}$	0.086	59	$d_{xy} + d_{xy}$
$5e_g$	0.307	68	$d_{xz} + d_{xz}$	$5e_g{}^a$	0.097	54	$d_{xz} + d_{xz}$
$1a_{1u}{}^a$	0.343	0		$1a_{1u}$	0.151	0	
$1a_{2g}$	0.343	0		$1a_{2g}$	0.151	0	
$5e_u$	0.352	0		$2b_{2u}$	0.163	0	
$2b_{2u}$	0.353	0		$5e_u$	0.163	0	
$4e_g$	0.354	0		$4e_g$	0.165	0	
$4a_{2u}$	0.355	0		$4e_u$	0.168	0	
$4e_u$	0.355	0		$2b_{1g}$	0.169	0	
$2b_{1g}$	0.357	0		$4a_{2u}$	0.171	0	
$3e_g$	0.368	5		$3a_{1g}$	0.192	2	
$3a_{1g}$	0.374	3		$3e_g$	0.193	6	
$3e_u$	0.376	2		$3e_u$	0.201	6	
$2e_g$	0.412	13		$2e_g$	0.219	16	
$2e_u$	0.426	9		$2e_u$	0.250	7	
$3a_{2u}$	0.449	13		$1b_{1u}$	0.268	38	$d_{xy} - d_{xy}$
$1e_g$	0.462	48	$d_{xz} + d_{xz}$	$1b_{2g}$	0.270	38	$d_{xy} + d_{xy}$
$1b_{1u}$	0.468	50	$d_{xy} - d_{xy}$	$3a_{2u}$	0.279	12	
$1e_u$	0.487	44	$d_{xz} - d_{xz}$	$1e_g$	0.280	23	$d_{xz} + d_{xz}$
$2a_{1g}$	0.489	25	$d_{z^2} + d_{z^2}$	$1e_u$	0.297	31	$d_{xz} - d_{xz}$
$2a_{2u}$	0.506	46	$d_{z^2} - d_{z^2}$	$2a_{2u}$	0.305	31	$d_{z^2} - d_{z^2}$
$1a_{1g}$	0.511	40	$d_{z^2} + d_{z^2}$	$2a_{1g}$	0.306	31	$d_{z^2} + d_{z^2}$
$1b_{2g}$	0.519	48	$d_{xy} + d_{xy}$	$1b_{2u}$	0.307	43	$d_{x^2-y^2} - d_{x^2-y^2}$
$1b_{2u}$	0.519	48	$d_{x^2-y^2} - d_{x^2-y^2}$	$1b_{1g}$	0.308	43	$d_{x^2-y^2} + d_{x^2-y^2}$
$1b_{1g}$	0.519	48	$d_{x^2-y^2} + d_{x^2-y^2}$	$1a_{1g}$	0.321	24	$d_{z^2} + d_{z^2}$
$1a_{2u}$	0.577	44	$d_{z^2} - d_{z^2}$	$1a_{2u}$	0.379	38	$d_{z^2} - d_{z^2}$

[a] The highest occupied level.

TABLE 3

Energies (Ry) and Metal Contributions of the Ground-State Upper Valence Levels for $[Mo_2O_{10}]^{12-}$

Level	$-E$ (Ry)	$2Q_{Mo}$ (%)	Major Mo (l,m)	Level	$-E$ (Ry)	$2Q_{Mo}$ (%)	Major Mo (l,m)
$4b_{3g}$	0.067	62	$d_{yz} + d_{yz}$	$2b_{2g}$	0.353	0	
$5b_{3u}$	0.076	out		$3b_{3u}$	0.354	1	
$7a_g$	0.115	out		$2b_{3u}$	0.386	1	
$3a_{1u}$	0.117	60	$d_{xz} - d_{xz}$	$4a_g$	0.404	4	
$4b_{2g}$	0.121	46	$d_{xz} + d_{xz}$	$2b_{1u}$	0.418	4	
$5b_{1u}$[a]	0.147	50	$d_{yz} - d_{yz}$	$2b_{1g}$	0.418	4	
$6a_g$	0.218	51	$d_{x^2-y^2} + d_{x^2-y^2}$	$3a_g$	0.427	9	
$3b_{3g}$	0.271	6		$3b_{2u}$	0.430	9	
$5b_{2u}$	0.273	1		$1b_{3g}$	0.481	20	$d_{yz} + d_{yz}$
$3b_{2g}$	0.282	0		$1a_u$	0.498	23	$d_{xz} - d_{xz}$
$4b_{1g}$	0.285	2		$2b_{2u}$	0.505	24	$d_{z^2} - d_{z^2}$
$2b_{3g}$	0.294	6		$2a_g$	0.511	27	$d_{z^2} + d_{z^2}$
$4b_{2u}$	0.296	4		$1b_{1g}$	0.527	31	$d_{xy} + d_{xy}$
$4b_{1u}$	0.299	2		$1b_{2g}$	0.570	24	$d_{xz} + d_{xz}$
$2a_u$	0.314	3		$1b_{2u}$	0.574	28	$d_{x^2-y^2} - d_{x^2-y^2}$
$3b_{1u}$	0.322	2		$1b_{1u}$	0.575	30	$d_{yz} - d_{yz}$
$3b_{1g}$	0.322	0		$1b_{3u}$	0.582	31	$d_{xy} - d_{xy}$
$4b_{3u}$	0.323	3		$1a_g$	0.588	37	$d_{x^2-y^2} + d_{x^2-y^2}$
$5a_g$	0.326	4					

[a] The highest occupied level.

tinctly separated into several categories. We shall discuss the arrangement of the levels in detail only for $[Mo_2O_{11}]^{14-}$ and $[Mo_2O_{10}]^{12-}$ since the features of the level diagram of $[Mo_2O_{11}]^{10-}$ are close to that of $[Mo_2O_{11}]^{14-}$ except for the shift of all the levels due to different number of electrons and some insignificant interior rearrangements of the order of levels inside each category. Roughly in order of increasing energy we can distinguish the following categories of levels: (1) levels having 20–40% Mo character, the main contributors to covalent Mo–O bonding; they are 12 in number in the range -0.268 to -0.379 Ry for $[Mo_2O_{11}]^{14-}$ and 10 in number in the range of -0.481 to -0.588 Ry for $[Mo_2O_{10}]^{12-}$. Electrons occupying those levels form the bonds between molybdenum and oxygen atoms in excellent agreement with the number of bonds expected on the basis of simple geometrical considerations. (2) A number of closely spaced levels having 90–100% oxygen character, 21 levels in the range -0.151 to -0.279 Ry in the former case and 20 levels in the range -0.271 to -0.430 in the latter one, representing nonbonding oxygen electrons and contributors to ionic Mo–O bonding. (3) Levels having 40–60% Mo character composed of mostly metal $4d$ orbitals.

These latter levels are considered for special attention because of the possibility of direct Mo–Mo bond formation in the case of $[Mo_2O_{10}]^{12-}$. In $[Mo_2O_{11}]^{14-}$ only one of these levels, $5e_g$ with energy -0.097 Ry, is occupied by four electrons and it is antibonding with respect to the Mo–Mo interaction. In the second case the situation is rather different. The first orbital from this group, $6a_g$ (-0.218 Ry), is the bonding combination of Mo $d_{x^2-y^2}$ orbitals with 51% Mo character and is essentially the occupied σ component of the Mo–Mo bond. The last occupied orbital, $5b_{1u}$ with energy -0.147 Ry, is the bonding combination of d_{yz} orbitals with 50% Mo character and forms the π component of the Mo–Mo bond. The bonding character of these two orbitals is obvious—they are clearly sepa-

rated from the top of the O 2*p* band as well as from the bottom of the virtual levels. The bonding–antibonding energy gap for $\pi(d_{yz} - d_{yz}) - \pi^*(d_{yz} + d_{yz})$ equals 1.1 eV whereas in the σ–σ^* case the energetic separation is much larger so that $\sigma^*(d_{x^2-y^2} - d_{x^2-y^2})$ has been eliminated from the diagram since it is of positive energy (this indicates that the σ–σ^* separation is larger than 3 eV). The next virtual orbitals may be regarded as unoccupied δ, δ^*, and π^* counterparts to the bonding ones; the remaining two orbitals, $7a_g$ and $5b_{3u}$, seem to be antibonding counterparts of the Mo–O bonding orbitals in category I with diffused outer-sphere characters. One thus has a rather classic energy-level diagram for a transition metal complex in the upper valence region in order of increasing energy, metal–ligand bonding, nonbonding and metal–ligand antibonding orbitals, except that the last are severely perturbed by being strongly bonding with respect to metal–metal interactions.

The wavefunction contour plots for the two highest occupied orbitals in $[Mo_2O_{10}]^{12-}$ are presented in Figs. 2 and 3 in order to show the effective Mo–Mo bonding directly. The first contour diagram (Fig. 2) shows that $6a_g$ MO consists mainly of Mo $4d_{x^2-y^2}$ orbitals resulting in the main component of the Mo–Mo σ bond. The $5b_{1u}$ level is strongly Mo–Mo π bonding as can be qualitatively seen from Fig. 3. The dashed lines represent negative wavefunction values. The outermost contours have the values ±0.0236 with the contour spacing equal to 0.0231.

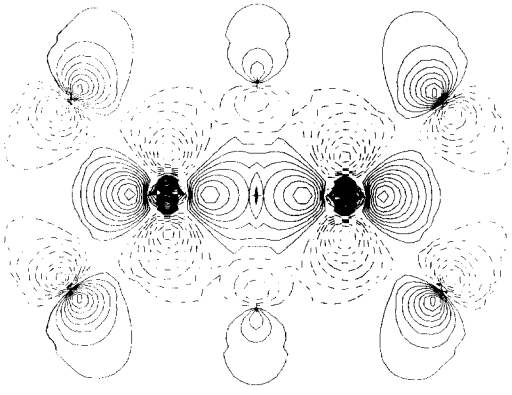

FIG. 2. Contour plot of $6a_g$ wavefunction values for $[Mo_2O_{10}]^{12-}$ in *xy* plane. The outermost contours have the values ±0.0236, with the contour spacing equal to 0.0231. Dashed lines represent negative wavefunction values.

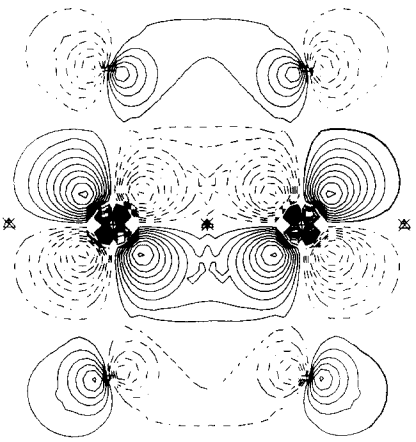

FIG. 3. Contour plot of $5b_{1u}$ wavefunction values for $[Mo_2O_{10}]^{12-}$ in *yz* plane. The same contour values as in Fig. 2.

4. CORE-LEVEL IONIZATION POTENTIALS AND THEIR INTERPRETATION

The SCF–SW–Xα method with addition of Slater's "transition-state" concept (*7*) gives ionization potentials generally in better agreement with experiment than semiempirical calculations (*21, 22*). Therefore one of our purposes was to calculate Mo 3*d* ionization potentials for the series of molybdenum oxides with different oxidation number of the metal central atom and different structures and to compare them with experimental ESCA results. We calculated the corresponding binding energies by performing the self-consistent procedure after removal of 0.5 electron from the level under consideration. Since the calculations were performed in a spin-restricted manner we did not obtain the splitting between the $3d_{3/2}$ and the $3d_{5/2}$ doublet. The results of our present calculations are listed and compared with our previous work (*5*) and the

experimental data of Haber *et al.* (*9a*) in Table 4. The effect of enlarging the size of the cluster is obvious. Our present results differ only by 2 eV (~1%) from the values of ionization potentials obtained in solid-state measurements by means of ESCA spectroscopy, whereas the simple octahedra calculations (*5*) gave discrepancies of over 6 eV. On the other hand double-octahedral cluster calculations give the possibility of further understanding of the molybdenum oxide reduction process and of drawing a more realistic interpretation of the phenomena observed. The real structure (*16*) of MoO_3 consists of strings of octahedra which are linked mostly by corners whereas in the case of MoO_2 there appear clusters of edge-sharing octahedra. In the latter arrangement the distance between the two molybdenum ions decreases and it is possible to form a bond between the two paired Mo^{4+} ions. Thus the inner-shell ESCA spectra obtained in the different steps of the reduction process may be ascribed as follows: (1) the spectrum of pure MoO_3 represented by two Mo^{6+} ions surrounded by two corner-linked oxygen octahedra; (2) the spectrum of slightly reduced MoO_3 represented by two Mo^{4+} ions surrounded by the same arrangement of oxygen ions; and (3) the spectrum of MoO_2 represented by two Mo^{4+} ions surrounded by two edge-linked octahedra. The first shift of the Mo 3*d* binding energy should be therefore due to the change of the formal molybdenum oxidation number followed by the change of electron density whereas the second shift should be due to the molybdenum–molybdenum bond formation.

TABLE 4

Mo 3*d* Ionization Potentials (eV) as Given by Experiment (9), Calculated within the Single-Octahedron Model (5) and Obtained in the Present Work

Experiment		Theoretical results for single octahedron		Theoretical results for double octahedra	
234.7	Mo^{6+}	240.9	$[MoO_6]^{6-}$	233.3	$[Mo_2O_{11}]^{10-}$
233.2	Mo^{4+}	239.0	$[MoO_6]^{8-}$	231.3	$[Mo_2O_{11}]^{14-}$
231.4	Mo^{2+}	237.8	$[MoO_6]^{10-}$	228.8	$[Mo_2O_{10}]^{12-}$

5. DISCUSSION

Our results presented in the previous two sections seem to create a fairly good picture of the electronic structure and chemical bonding in molybdenum oxides. It was expected that the enlargement of the cluster's size would improve the agreement of the calculated ionization potentials with experiment. Introduction of clusters composed of two octahedra allows more possibilities for investigations of the influence of the structure and gives a more realistic model of the real structure of the solid state as well. On the other hand metal–metal bond formation has become recognized as one of the most distinctive features in the chemistry of lower-oxidation-state transition metals. We tried to establish if such a phenomenon occurs in the MoO_2 case and the data obtained seem to indicate a positive answer on this question. In the cited paper of Haber *et al.* (*9a*) the interpretation of the photoelectron spectroscopy results for reduced MoO_3 involving the formation of Mo^{4+} and Mo^{2+} ions was suggested and our previous simplified calculations (*5*) supported this idea. The present paper may be also regarded as a more detailed contribution into the current discussion (*23, 24*) on the relationship between 3*d* binding energy and oxidation state in molybdenum oxides, dealing as it does with better developed models in a more quantitative way. On the basis of the present results we can draw much better the conclusion that due to the bond formation between the two paired Mo^{4+} ions the effective charge of each molybdenum ion may be regarded as corresponding to the apparent oxidation number of +2.

The SCF–SW–Xα calculation, despite its shortcomings, has helped us to arrive at a consistent correlation of the ESCA spectra and bonding in molybdenum oxides. We feel that the total picture of the electronic

structure of the oxides under consideration is reasonable and internally consistent provided that the crucial contribution to the electronic structure of these systems is the participation of metal atom *d* orbitals in the formation of molecular orbitals whose primary role is to bind the metal atoms together.

ACKNOWLEDGMENT

We wish to thank Professor D. R. Salahub for helpful discussions on this problem.

REFERENCES

1. Cotton, F. A., *J. Less Common Metals* **54,** 3 (1977); *Chem. Soc. Rev.* **4,** 27 (1975).
2. Norman, J. G., Jr., and Kolari, H. J., *J. Amer. Chem. Soc.* **97,** 33 (1975).
3. Chisholm, M. H., Cotton, F. A., Extine, M. W., and Kelly, R. L., *J. Amer. Chem. Soc.* **101,** 7645 (1979).
4. Chisholm, M. H., Cotton, F. A., Extine, M. W., and Reichert, W. W., *Inorg. Chem.* **17,** 2944 (1978).
5. Broclawik, E., Foti, A. E., and Smith, V. H., Jr., *J. Catal.* **51,** 380 (1978).
6. Slater, J. C., and Johnson, K. H., *Phys. Rev. B* **5,** 844 (1972).
7. Slater, J. C., *Advan. Quant. Chem.* **6,** 1 (1972).
8. Johnson, K. H., *Advan. Quant. Chem.* **7,** 143 (1973).
9. (a) Haber, J., Marczewski, W., Stoch, J., and Ungier, L., *Ber. Bunsenges. Phys. Chem.* **79,** 970 (1975); (b) Haber, J., *J. Less Common Metals* **54,** 243 (1977).
10. Swartz, W. E., and Hercules, D. M., *Anal. Chem.* **43,** 1774 (1971).
11. Cimino, A., and de Angelis, B. A., *J. Catal.* **36,** 11 (1975).
12. Gubanov, V. A., Webber, J., and Connolly, J. W. D., *Chem. Phys.* **11,** 319 (1975).
13. Gubanov, V. A., and Ellis, D. E., *J. Struct. Chem. (USSR)* **17,** 826 (1977).
14. Gupta, M., Gubanov, V. A., and Ellis, D. E., *J. Phys. Chem. Solids* **38,** 499 (1977).
15. Gubanov, V. A., Ellis, D. E., and Fotiev, A. A., *J. Solid State Chem.* **21,** 303 (1977).
16. Kihlborg, L., *Ark. Kemi* **21,** 443 (1963).
17. Magneli, A., *Acta Chem. Scand.* **11,** 28 (1957).
18. Slater, J. C., "Quantum Theory of Molecules and Solids," Vol. 2. McGraw-Hill, New York, 1965.
19. Watson, R. E., *Phys. Rev.* **111,** 1108 (1958).
20. Schwartz, K., *Phys. Rev. B* **5,** 2466 (1972); *Theor. Chim. Acta* **34,** 225 (1974).
21. Connolly, J. W. D., *Int. J. Quant. Chem.* **6,** 201 (1972).
22. Rösch, N., Smith, V. H., Jr., and Whangbo, M. H., *J. Amer. Chem. Soc.* **96,** 5984 (1974); *Inorg. Chem.* **15,** 1768 (1976).
23. Cimino, A., and de Angelis, B. A., *J. Catal.* **62,** 182 (1980).
24. Broclawik, E., Foti, A. E., and Smith, V. H., Jr., *J. Catal.* **62,** 185 (1980).